Designer spin systems via inverse statistical mechanics. II. Ground-state enumeration and classification

Étienne Marcotte,[1] Robert A. DiStasio, Jr.,[2] Frank H. Stillinger,[2] and Salvatore Torquato[1,2,3,4]
[1]*Department of Physics, Princeton University, Princeton, New Jersey 08544, USA*
[2]*Department of Chemistry, Princeton University, Princeton, New Jersey 08544, USA*
[3]*Princeton Institute for the Science and Technology of Materials, Princeton University, Princeton, New Jersey 08544, USA*
[4]*Program in Applied and Computational Mathematics, Princeton University, Princeton, New Jersey 08544, USA*
(Received 15 August 2013; published 27 November 2013)

In the first paper of this series [DiStasio, Jr., Marcotte, Car, Stillinger, and Torquato, Phys. Rev. B **88**, 134104 (2013)], we applied inverse statistical-mechanical techniques to study the extent to which targeted spin configurations on the square lattice can be ground states of finite-ranged radial spin-spin interactions. In this sequel, we enumerate all of the spin configurations within a unit cell on the one-dimensional integer lattice and the two-dimensional square lattice up to some modest size under periodic boundary conditions. We then classify these spin configurations into those that can or cannot be unique classical ground states of the aforementioned radial pair spin interactions and found the relative occurrences of these ground-state solution classes for different system sizes. As a result, we also determined the minimal radial extent of the spin-spin interaction potentials required to stabilize those configurations whose ground states are either unique or degenerate (i.e., those sharing the same radial spin-spin correlation function). This enumeration study has established that unique ground states are not limited to simple target configurations. However, we also found that many simple target spin configurations cannot be unique ground states.

DOI: 10.1103/PhysRevB.88.184432 PACS number(s): 05.20.−y, 05.50.+q, 05.65.+b, 75.10.Hk

I. INTRODUCTION

Interactions between the atomic or molecular particles contained in condensed phases produce an enormous diversity of geometric structures and resulting material properties. This diversity is of incalculable value to technology, while presenting fascinating scientific challenges to the research community for interpretation. This paper reports analytical and computational results extending an initial investigation that focused on geometric pattern production in classical spin system ground states.[1] Because the present work and its predecessor basically involve starting with a given *target* pattern, then searching for an optimal radial interaction function to attain that pattern as a classical ground state, the central strategy utilized has been classified as belonging to "inverse statistical mechanics."[2–7]

As in the preceding paper,[1] attention here focuses on static polarization patterns that can be exhibited by arrays of interacting Ising spins $\sigma_i = \pm 1$ $(1 \leqslant i \leqslant N)$ on a d-dimensional lattice, in the absence of external fields. The N spins constitute a finite unit cell that is periodically replicated over the infinite lattice; that is, this cluster of N spins is subject to periodic boundary conditions. In the cases to be examined here, the lattices are Bravais lattices, and therefore all spin locations are geometrically identical.

Ising models have a venerable history, introduced originally to explain the phenomenon of ferromagnetism.[8,9] Although the early versions of the Ising model considered only interactions between nearest neighbors on the lattice of interest,[8,10–12] subsequent investigations have extended the analysis to incorporate longer-ranged interactions.[13–19] Assuming that the interactions among the Ising spins are pairwise-additive and radial (i.e., isotropic), the total interaction energy E for the unit cell can be represented as follows:

$$E(\sigma_1, \ldots, \sigma_N) = -\sum_{i<j} J(R_{ij})\sigma_i\sigma_j, \tag{1}$$

where the sum covers all of the interactions of the N spins in the unit cell[20] and R_{ij} stands for the scalar distance between the i, j spin pair. Because the spins and their periodic images reside on a lattice, all possible distances R_{ij} form a discrete set. The summation in Eq. (1) includes all distances in that set up to a cutoff value R_C beyond which $J(R_{ij})$ becomes identically zero.

A basic descriptor for any single spin pattern on a lattice is the following spin-spin correlation function defined for the discrete set of interspin distances occurring on the lattice:

$$S_2(R) \equiv \frac{1}{N}\sum_{i<j} \sigma_i\sigma_j\delta_{R,R_{ij}}, \tag{2}$$

in which $\delta_{R,R_{ij}}$ is a generalized Kronecker delta.[21] This definition permits the energy per spin ϵ, for any spin pattern, to be simply written as

$$\epsilon \equiv \frac{E}{N} = -\sum_{R>0}^{R_C} J(R)S_2(R). \tag{3}$$

The fact that the spin-spin interaction potentials to be considered herein only depend on scalar distances implies that the energy per spin ϵ can experience pattern degeneracies. Some of these are trivial, arising from various pattern symmetries (boundary conditions permitting), such as translations, rotations, spatial and spin inversions, and combinations thereof. In addition there can arise pairs (or larger numbers) of distinct spin patterns not related by symmetry that happen to

possess identical $S_2(R)$ correlation functions for all R, specific examples of which have been previously identified.[1] If that is the case, then ϵ will be identical for these distinct patterns regardless of the spin-spin interaction potential $J(R)$. We will call the set of all Ising spin configurations on a given underlying lattice that possess the same $S_2(R)$ function an "iso-S_2 set." The elements of an iso-S_2 set that are related by combinations of symmetry operations will simply be regarded as trivial degeneracies. By contrast, the largest subset of spin patterns (configurations) in an iso-S_2 set that are not related to one another by the aforementioned symmetry operations will be identified as "nontrivial degeneracies." Throughout the remainder of this paper, any allusion to degenerate spin configurations will in fact refer to nontrivial degeneracies, the number of which is denoted by Ω for any given iso-S_2 set.

With respect to Ising model energy degeneracies, an historical note may be of passing interest. Specifically, the two-dimensional Ising models with nearest-neighbor antiferromagic interactions [$J(1) < 0$] on both the triangular Bravais lattice[22] and on the non-Bravais kagomé lattice[23] have ground states with high-order degeneracies. In fact, these degeneracies confer positive residual entropies on the ground states in the infinite-system size limit. However, these antiferromagnetic situations do not conform to the type of pattern analysis implemented in this paper, where finite Ising spin patterns are periodically replicated, and where spin-spin interaction potentials $J(R)$ are sought to produce nondegenerate ground states when possible.

In Ref. 1, we classified target spin configurations according to three solution class designations. In terms of the iso-S_2 formalism just introduced, these solutions classes can be equivalently restated as follows: (1) Class I: An iso-S_2 set with no (nontrivial) degeneracies for which a spin-spin interaction potential $J(R)$ can be constructed for which the iso-S_2 set is a corresponding unique ground state; (2) Class II: An iso-S_2 set exhibiting two or more (nontrivial) degeneracies for which a spin-spin interaction potential $J(R)$ can be constructed such that the energy per spin ϵ for each member of the iso-S_2 set is lower than that of all configurations outside the set; and (3) Class III: Any iso-S_2 set that belongs to neither class I nor class II. The latter is equivalent to stating that any iso-S_2 set for which any assigned interaction $J(R)$ produces a higher energy per spin, or an equal energy per spin, compared to spin configurations from at least one other set, belongs to class III.

The principal objective of this paper is to separate all possible iso-S_2 sets of spin configurations of a given unit cell size into those that can be unique classical ground states with an energy of the form Eq. (1), from those that cannot. The total number of possible spin patterns for a system containing N spins is 2^N (many of which are trivial degeneracies), thereby limiting the exhaustive searches considered in this work to modest system sizes. For the $d = 1$ integer lattice, we considered systems as large as $N = 21$, while for the $d = 2$ square lattice, we have considered both square and rectangular unit cells, the largest of which contains $N = 25$ spins in a 5×5 unit cell. In spite of the modest sizes of the unit cells examined herein, it is worth noting that population trends for the three distinct solution classes can still be identified as N increases.

In this investigation, we have obtained lower bounds on Ω for the iso-S_2 sets, which are sharp for all of the 1D integer and for most of the 2D square lattice sets, and have uncovered the relationship between Ω and system size for spin configurations on the 1D integer lattice. Using these enumeration results, we have employed inverse statistical-mechanical techniques to assign solution class designations (class I, II, or III) corresponding to each of the iso-S_2 sets and have found their relative occurrences for different system sizes. In doing so, we also determined the minimal radial extent of the spin-spin interaction potentials required to stabilize iso-S_2 sets belonging to classes I and II. In this paper, we show that inverse statistical-mechanical techniques can successfully create radial spin-spin interactions for which spin configurations with minimal symmetry are the unique classical ground states. The existence of these unique ground states opens the field of inverse methods toward much more unusual targets than have previously been studied in both spin[1] and many-particle systems,[2–7] which could aid in the design of materials with desired properties. By contrast, we demonstrate that many candidate targets cannot be the unique classical ground states of any set of radial spin-spin interactions, either due to S_2-type degeneracies (class II), or from guaranteed non-S_2-type degeneracies (class III).

The subsequent sections in this paper are arranged as follows. Section II presents a detailed description of the methods used to search for energy-minimizing isotropic interactions, and to identify spin patterns and their corresponding interaction potentials according to the class I, II, and III criteria stated above. Section III describes in detail the extensive results generated by our method for the modest-size systems examined on the integer and square lattices with periodic boundary conditions. The final section, Sec. IV, contains the discussion and conclusions, specifically including our estimates of the most productive directions in which future research regarding these pattern-controlling phenomena might proceed.

II. METHODS

This section is dedicated to the description of the various technical aspects of this research. In Sec. II A, we define both of the underlying lattices considered in this work: the one-dimensional (1D) integer and two-dimensional (2D) square lattices. In Sec. II B, we describe the protocol we have utilized to consider every spin configuration discretized on a given underlying lattice with a given periodicity. Finally, Sec. II C describes the inverse statistical-mechanical techniques that we employed to classify the different iso-S_2 sets and create spin-spin interaction potentials that correspond to ground states comprising the class I and II sets. These techniques have previously been employed in Ref. 1.

A. The integer ($\mathbb{Z}$) and square ($\mathbb{Z}^2$) lattices

A generalized Ising model with an energy defined according to Eq. (1) can be discretized on any given underlying lattice as long as the distance between any two spins is well-defined. Traditionally speaking, the Ising model has most often been studied on either the square or triangular lattices,[24,25] but investigations on more exotic networks, such as the Bethe

lattice and hyperbolic planes have also appeared in the literature.[26–28] In this paper, we restrict our investigation to the 1D integer lattice ($\mathbb{Z}$) and the 2D square lattice ($\mathbb{Z}^2$), with nearest-neighbor distances set to unity in both cases. On the integer lattice, the distance R_{ij} between spins σ_i and σ_j is simply

$$R_{ij} = |i - j|, \tag{4}$$

where i and j can take on any integer value. On the square lattice, the distance between spins is

$$R_{ij} = \sqrt{(x_i - x_j)^2 + (y_i - y_j)^2}, \tag{5}$$

in which the spin coordinates, $\{x_i, y_i\}$ and $\{x_j, y_j\}$, are also integers. Since both the integer and square lattices are periodic, this allows us to use periodic boundary conditions to approximate the infinite system limit.

Throughout this work, the size of the unit cell for a spin system discretized on the integer lattice will be denoted by n. For this case, the total number of spins, N, is therefore $N = n$ and the only allowed lattice vector is (n). In the same vein, the unit cell size for the square lattice will be denoted by $m \times n$, with $N = mn$ and corresponding lattice vectors taken as $(m,0)$ and $(0,n)$. Although unit cells characterized by lattice vectors that are not aligned with the $(1,0)$ and $(0,1)$ directions can also exist on the square lattice, this set of unit cells was not included in the present study. We note in passing that any spin configuration with such a unit cell can be equivalently represented by a larger unit cell with lattice vectors aligned with the aforementioned canonical directions.

B. Enumeration protocol

Unlike continuous point-particle systems, for which there exists an uncountably infinite number of configurations, the spin systems considered herein have discrete degrees of freedom (where each spin can only be $+1$ or -1), which allows for a finite number of spin configurations. We take advantage of this property and explicitly enumerate all spin configurations discretized on the 1D integer and 2D square lattices with specific unit cells. The total number of spin configurations that can be represented on a periodic underlying lattice with N spins contained within the unit cell is 2^N, since each spin can take on one of two distinct values. In order to obtain an accurate count of the number of iso-S_2 sets belonging to each solution class, it is necessary to enumerate all of the configurations belonging to each of these sets. To do so, we first compute the spin-spin correlation function, $S_2(R)$, given in Eq. (2), for all of the 2^{N-1} spin configurations (using spin-inversion symmetry to fix one of the spins reduces the total number of spin configurations by a factor of 2), and store the list of possible $S_2(R)$ functions. Throughout this work, $S_2(R)$ is computed up to the first 100 coordination shells for both of the underlying lattices; however, we have found that the first differing value of $S_2(R)$ (for non-S_2-degenerate spin configurations) always occurs at a radial distance smaller than, or of the order of, the periodicity of the spin configurations in question.

This enumeration method was also adapted to compute the number of nontrivial degeneracies Ω in each iso-S_2 set. In this case, instead of only storing the $S_2(R)$ function for a given iso-S_2 set, we also store a running list of the nontrivial degeneracies contained in this set. Whenever a new spin configuration that is characterized by a previously stored spin-spin correlation function is encountered during the enumeration process, we are left with the task of determining

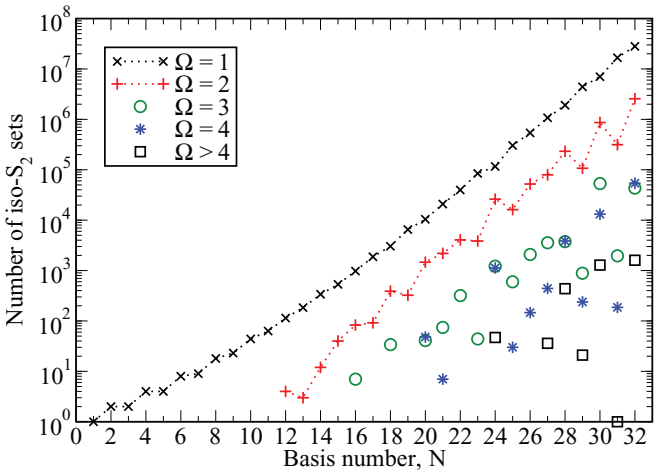

FIG. 1. (Color online) The number of iso-S_2 sets which contains a certain number Ω of degenerate spin configurations for spin configurations discretized on the 1D integer lattice with a N spin basis (omitted symbols indicate that no sets have such values of Ω for the given N). For a given N, all sets which contain at least one configuration that can be represented using N periodic spins are included in the enumeration of Ω. A consequence of this is that the class I ferromagnetic set (with all spins aligned) is included in $\Omega = 1$ for all N.

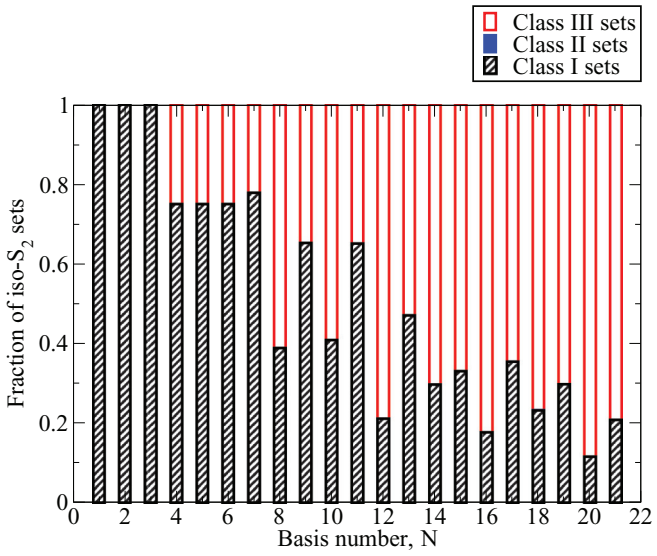

FIG. 2. (Color online) The relative amount of iso-S_2 sets that are in classes I, II, or III, for spin configurations discretized on the 1D integer lattice with an N spin basis. Although it is essentially imperceptible in this figure, we found two class II sets for $N = 18$ (out of a total of 3456 sets). These two sets are depicted in Fig. 3. Even though the first class II sets were found at $N = 18$, this does not mean that there are no S_2 degeneracies for smaller systems. As seen in Fig. 1, there are doubly-degenerate sets ($\Omega = 2$) starting at $N = 12$. However, for $12 \leqslant N \leqslant 17$, all of these sets belong to class III. We have also found 18 class II iso-S_2 sets for $N = 21$ (out of a total of 23 121).

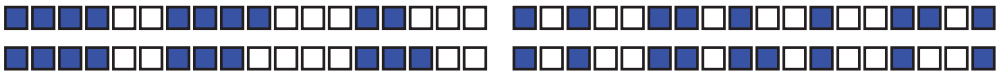

(a) (b)

FIG. 3. (Color online) The two class II iso-S_2 sets found among 18-spin configurations discretized on the 1D integer lattice, each with a degeneracy $\Omega = 2$.

whether or not this configuration is a trivial or nontrivial degeneracy with respect to the members of the corresponding iso-S_2 set. Such a determination can be achieved by comparing the spin configuration to *each* member of the given iso-S_2 set and performing a spin-by-spin check for symmetrical equivalence up to translations, rotations, reflections, and spin inversion. By updating the list with all of the nontrivial degeneracies found, the number of configurations in the list at the end of the enumeration process yields Ω for each iso-S_2 set. However, one apparent weakness of this method is that it fails to identify any of the S_2-degeneracies corresponding to spin configurations that cannot be represented on the unit cell considered during the enumeration; hence, the values of Ω computed utilizing this protocol are strictly lower bounds (see Figs. 6 and 7 for illustrative examples).

C. Generation and verification of spin-spin interaction potentials

Throughout this work, we follow the method first employed in Ref. 1 to generate spin-spin interaction potentials, $J(R)$, which yield ground states that are contained within single iso-S_2 sets (i.e., class I and II solutions), or to disprove the existence of any such potential (i.e., class III solutions). Given a spin configuration $\mathscr{T}$ from a targeted iso-S_2 set and a competitor spin configuration C from another iso-S_2 set, the difference in energy per spin between these configurations can be written as

$$\Delta\epsilon^C \equiv \epsilon^C - \epsilon^{\mathscr{T}} = -\sum_R J(R)\left[S_2^C(R) - S_2^{\mathscr{T}}(R)\right], \quad (6)$$

which is clearly a linear function of the interaction potential $J(R)$ for each of the interspin separations allowed by the underlying lattice. In order for $\mathscr{T}$ to be the unique ground state corresponding to $J(R)$, $\Delta\epsilon^C$ must be positive for *all* possible competitors C. Since such a calculation is intractable, we instead select the potential which maximizes $\Delta\epsilon^C$ between the target and the competitor(s) that are closest in energy via

$$z \equiv \max_{J(R)} \left(\min_C \Delta\epsilon^C \right), \quad (7)$$

in which z is the objective function. Here, the maximization is performed over all allowed potentials, and the minimization is performed over the set of known competitors.

Equations (6) and (7) can both be expressed as inequalities that are linear in z and $J(R)$. Therefore standard linear programming techniques, such as the simplex algorithm, can be used to efficiently find the global optimum value of the objective function. However, the problem as defined above is not bounded, since multiplying all of the $J(R)$ and z by a positive constant has no effect on the inequalities. Therefore, if we already have a valid solution with a positive z value, we could generate solutions with arbitrarily large z values. To solve this issue, we bound all of the $J(R)$ to be in the range: $[-1, +1]$. Such bounded $J(R)$ functions can reproduce any possible interaction potential, up to the aforementioned positive constant.

The potential $J(R)$ is also set to zero for all R larger than some radial cutoff distance R_C, initially set at $R_C = 1$. If the objective function z is identically zero, then this is indicative of the fact that it is impossible for $\mathscr{T}$ to be the unique ground state for any potential $J(R)$ under the given restrictions, since at least one $\Delta\epsilon^C$ will be nonpositive for any potential. In this situation, we relax this restriction on R_C by incrementing R_C to the next smallest distance allowed by the underlying lattice and recalculate z. This ensures that our optimization algorithm will find the shortest possible potential for the given target spin configuration. If z remains zero even when allowing for potentials much longer than the periodic cell size, this signifies that $\mathscr{T}$ cannot be a unique ground state, and therefore belongs to class III. If z is positive, we have obtained a putative potential $J(R)$ for which we must confirm that $\mathscr{T}$ is indeed the corresponding ground state. To do so, we repeatedly use

TABLE I. The spin-spin interaction potentials $J(R)$ corresponding to the two class II iso-S_2 sets shown in Fig. 3. All configurations from both sets have a $N = 18$ spin basis and a potential cutoff of $R_C = 15$. The corresponding spin-spin correlation functions $S_2(R)$ and the energies per spin ϵ are also shown for comparison. Both sets are related through a gauge transformation since the spin configurations from Fig. 3(a) can be transformed to the spin configurations from Fig. 3(b) by inverting every other spin $[\sigma_i \to (-1)^i\sigma_i]$. This same transformation leads to a S_2 and potential function which have opposite sign for every odd R $[S_2(R) \to (-1)^R S_2(R)$ and $J(R) \to (-1)^R J(R)]$.

	Figure 3(a)		Figure 3(b)	
R	$J(R)$	$S_2(R)$	$J(R)$	$S_2(R)$
1	1	1/3	−1	−1/3
2	−1	−1/3	−1	−1/3
3	0.857	−5/9	−0.857	5/9
4	−0.806	−1/3	−0.806	−1/3
5	1	1/3	−1	−1/3
6	−0.714	5/9	−0.714	5/9
7	1	1/3	−1	−1/3
8	−1	−1/3	−1	−1/3
9	0.429	−7/9	−0.429	7/9
10	−0.516	−1/3	−0.516	−1/3
11	0.608	1/3	−0.608	−1/3
12	−0.286	5/9	−0.286	5/9
13	0.887	1/3	−0.887	−1/3
14	−0.427	−1/3	−0.427	−1/3
15	0.143	−5/9	−0.143	5/9
ϵ	−1.303		−1.303	

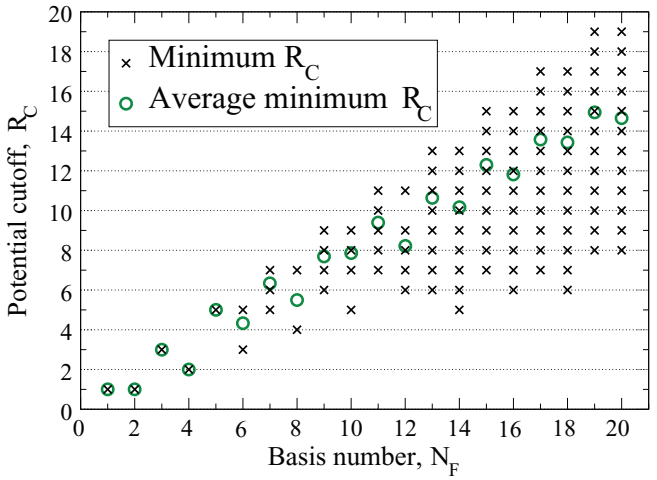

FIG. 4. (Color online) The minimal range R_C of the spin-spin interaction potentials required to stabilize spin configurations discretized on the 1D interger lattice in term of N_F, the number of spins in the respective fundamental cells. The circles indicate the average R_C for all configurations with the same fundamental cell size.

a simulated annealing (SA) procedure using the Metropolis algorithm to relax disordered spin configurations with variable periodic unit cells ($1 \leqslant n \leqslant 100$ for the integer lattice, and $1 \leqslant m \leqslant n \leqslant 30$ for the square lattice). If a spin configuration is found that has an energy per spin that is lower than or equal to $\epsilon^{\mathscr{T}}$, but with a different $S_2(R)$ spin-spin correlation function, then this disproves the putative potential $J(R)$. This spin configuration is then added to the list of known competitors, and the optimization is restarted. If we do not find any such competitors before the SA procedure yields the desired target ground state 100 times, then we have amassed sufficiently strong evidence that we have obtained a valid potential.

III. RESULTS

A. The 1D integer ($\mathbb{Z}$) lattice

The 1D integer lattice is a very simple yet consequence-rich model to study how the number of degeneracies and the ratio of iso-S_2 sets in the different solution classes vary with the system size. This simplicity is a direct result of the lattice having a single parameter (n) which describes the period of the spin configurations. Figure 1 shows how the number of iso-S_2 sets of a given degeneracy, Ω, increases with the basis number $N = n$, regardless of the solution class to which the set belongs. A first observation is that the number of iso-S_2 sets grows exponentially with N, which is relatively unsurprising considering the fact that the total number of spin configurations also grows exponentially as 2^N. The growth in the number of iso-S_2 sets is actually somewhat slower (approximatively proportional to 1.85^N), a consequence of the fact that the

FIG. 5. (Color online) The unique spin configuration on the 1D integer lattice with $N_F = 14$ spins in its fundamental cell which can be stabilized using a potential with cutoff $R_C = 5$. Table II presents one such spin-spin interaction potential.

TABLE II. The spin-spin interaction potential $J(R)$ corresponding to a ground state (in Fig. 5) which has $N_F = 14$ spins even though the potential has a relatively short cutoff at $R_C = 5$. The corresponding spin-spin correlation function $S_2(R)$ and energy per spin ϵ of the potential ground state are also shown.

R	1	2	3	4	5	ϵ
$J(R)$	$-2/9$	1	$2/3$	$-1/3$	$-4/9$	$-46/63$
$S_2(R)$	$1/7$	$3/7$	$1/7$	$-1/7$	$-3/7$	

number of trivial degeneracies also increases with N. A second observation is that the number of iso-S_2 sets with different degeneracies Ω apparently have the same rate of exponential growth. This indicates that, even in the infinite size limit, the vast majority of the sets remain nondegenerate ($\Omega = 1$).

This property is a peculiarity of the underlying integer lattice, for which the radially-averaged $S_2(R)$ function contains exactly the same information as the directional spin-spin correlation function $\widehat{S}_2(\mathbf{R})$, since $\widehat{S}_2(\mathbf{R}) = S_2(R = |\mathbf{R}|)$ for any vector and spin configuration discretized on the 1D integer lattice. In general, we can also define a directional spin-spin correlation function $\widehat{S}_2(\mathbf{R})$, which is more appropriate for anisotropic pairwise interactions:

$$\widehat{S}_2(\mathbf{R}) = \frac{1}{N} \sum_{ij} \sigma_i \sigma_j \delta_{\mathbf{R},\mathbf{R}_{ij}}, \tag{8}$$

where $\mathbf{R}_{ij}$ is the d-dimensional vector from spin i to spin j. The radial $S_2(R)$ can then be readily obtained from $\widehat{S}_2(\mathbf{R})$ by summing over all equal-length vectors:

$$S_2(R) = \frac{1}{2} \sum_{|\mathbf{R}|=R} \widehat{S}_2(\mathbf{R}), \tag{9}$$

where the $1/2$ factor corrects for the double counting in the definition of $\widehat{S}_2(\mathbf{R})$, since $\widehat{S}_2(-\mathbf{R}) = \widehat{S}_2(\mathbf{R})$.

A third observation (see Fig. 1) concerns those basis numbers at which the number of doubly-degenerate sets ($\Omega = 2$) is either decreasing or barely increasing: 13, 17, 19, 23, 25, 29, 31. These basis numbers are all of the prime numbers between 12 and 32 (25 being the only exception,

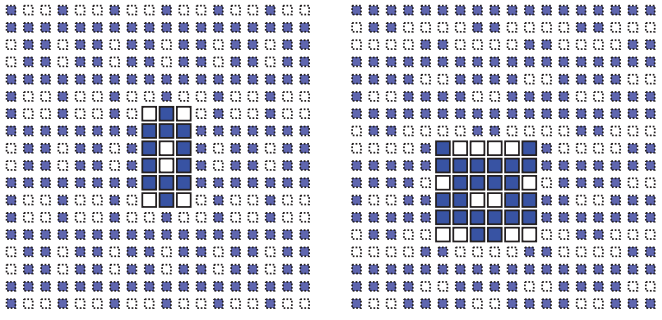

FIG. 6. (Color online) An example of two spin configurations that belongs to the same class II iso-S_2 set, and therefore have identical $S_2(R)$ functions, while having a different number of spins N_F in their fundamental cells. The spins in their fundamental cells are denoted using a solid outline, while other spins are denoted using a dashed outline and smaller squares. The number of spins in their fundamental cells are 18 and 36, respectively.

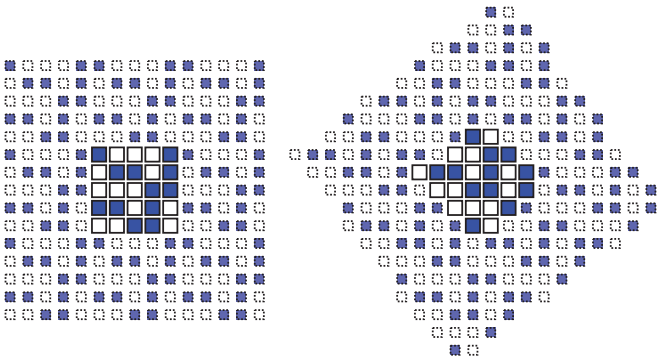

FIG. 7. (Color online) An example of two spin configurations that belongs to the same class II iso-S_2 set, and therefore have identical $S_2(R)$ functions, with differently-aligned fundamental cells. The fundamental cell of the left configuration has (5,0) and (0,5) as its basis vectors, while those of the right configuration are (4,3) and (3, − 4). The spins in their fundamental cells are denoted using a solid outline, while other spins are denoted using a dashed outline and smaller squares. Both have $N_F = 25$.

TABLE III. The number of iso-S_2 sets of spin configurations with a $m \times n$ basis in each solution class for the underlying 2D square lattice. For each m and n, the data are represented in the following manner: number of class I sets / number of class II sets / number of class III sets. It should be mentioned that all spin configurations which can be represented with the given basis are counted, even if they could also be represented using a smaller unit cell. For example, all 5 of the 4×4 class I configurations are also 2×4 configurations (see Fig. 12). We have also enumerated the sets with 4×6, 5×6, and 6×6 bases. There are respectively 48 914, 1 594 858, and 4 868 629 such sets.

	n					
m	1	2	3	4	5	6
1	1/0/0	2/0/0	2/0/0	3/0/1	3/0/1	6/0/2
2		3/0/1	6/0/2	5/0/15	18/0/26	23/0/104
3			3/2/6	15/1/65	37/2/221	31/19/1030
4				5/1/266	301/2/4666	
5					74/29/8209	

although it is a squared prime number). We have not studied the cause of this pattern, but it is plausible that the increased occurrence rate of symmetry for nonprime number bases is responsible for the observed trend.

Using the approach described in Sec. II C, we classified all iso-S_2 sets for the underlying 1D integer lattice with $N \leqslant 21$, either by generating a potential $J(R)$ for which the ground state is the specified set, or by proving that no such potential exists. Figure 2 shows the fraction of sets in each solution class for each basis number. The fact that this fraction for class I decreases overall with increased system size is also unsurprising considering the growing complexity that configurations with more spins can achieve. However, it is interesting to note that spin configurations with odd N usually have a higher fraction of class I sets than spin configurations with neighboring even N. Configurations with odd N being easier to stabilize is likely due to a broken symmetry, although its precise mechanism still needs to be understood.

In all of our calculations on the underlying 1D integer lattice, we have only discovered 20 class II iso-S_2 sets, 2 for $N = 18$ and 18 for $N = 21$. The $N = 18$ class II iso-S_2 sets are shown in Fig. 3. The spin-spin interaction potentials corresponding to these degenerate configurations as ground states are presented in Table I.

As mentioned in Sec. II C, the method utilized to generate spin-spin interaction potentials for a given iso-S_2 set only tries to obtain potentials with a given cutoff R_C after it has already been proved that all shorter potentials are unable to stabilize the set. Therefore any interaction potential $J(R)$ that the method returns is always going to have the shortest possible cutoff for the targeted set. This property allows us to explore the range limitations of generalized Ising spin-spin interactions. Figure 4 clearly shows the upper bound on the minimal value of the cutoff: $R_C \leqslant N_F$ if N_F is odd, and $R_C \leqslant N_F - 1$ if N_F is even, where N_F denotes the number of spins in the fundamental cell of a given spin configuration, where the fundamental cell is

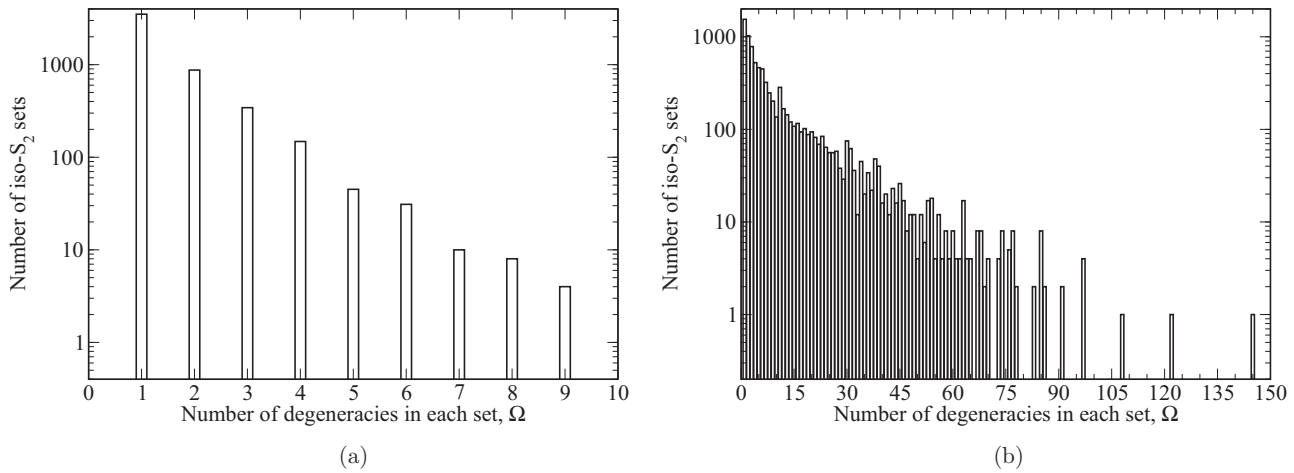

FIG. 8. The number of iso-S_2 sets which contains a certain number Ω of degeneracies for spin configurations discretized on the 2D square lattice with (a) a 4×5 basis and (b) a 5×5 basis. Only the degenerate spin configurations which can be represented using the exact same basis have been counted, thereby Ω is only guaranteed to be a lower bound in these cases.

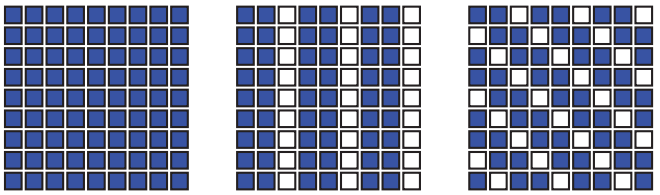

FIG. 9. (Color online) All class I spin configurations which can be represented using a 3×3 basis on the 2D square lattice. The middle spin configuration was previously reported in Ref. 1 as SP[1,2].

the smallest repeat unit in the spin configuration (which can be smaller than the unit cell). The $R_C \leqslant N_F$ upper bound can readily be proven via the following observation: for any spin configuration on the underlying 1D integer lattice with a periodic unit cell containing N spins, $S_2(R = N) = 1$, the maximum value that $S_2(R)$ can achieve on this lattice. Now, let us consider an interaction potential $J(R)$ such that its value at $R = N$ is much larger than all of its other values: $J(N) \gg |J(R)| \, \forall R \neq N$. Such an interaction potential will clearly favor spin configurations with $S_2(R = N) = 1$ over all others, so its ground state will be represented using a N spin basis. Since $S_2(R + N) = S_2(R)$ for such configurations, any potential longer than N can be shortened to $R_C = N$, without changing its ground state. Therefore the minimal cutoff R_C has a upper bound equal to N_F, the number of spins in the fundamental cell. The lower bound on R_C is more complex, since it deviates from $R_C \geqslant N_F/2$ as early as $N_F = 13$. Figure 5 shows one spin configuration which breaks that rule, since it has $N_F = 14$ spins in its fundamental cell yet it is the ground state of an interaction potential with a cutoff at $R_C = 5$ (see Table II).

B. The 2D square lattice

Unlike the spin configurations on the underlying 1D integer lattice studied in Sec. III A, spin configurations on an underlying 2D square lattice can have a wide variety of unit cell lattice vectors. While it is conceivable to enumerate all spin configurations that can be represented with a unit cell containing a specific number of spins, but with otherwise arbitrary lattice vectors, we elect to restrict our investigation in this work to spin configurations with unit cell lattice vectors that are aligned with the underlying square lattice. Figure 6 shows an example of two degenerate spin configurations with not only different fundamental cells, but also different numbers of spins N_F in their fundamental cells. Figure 7 shows another example of two degenerate spin configurations with different fundamental cells, which differ only by their orientation instead of by the number of spins. Both of these types of degeneracies will not be identified when computing Ω using brute force enumeration of the spin configurations discretized on a given unit cell. However, when determining whether an iso-S_2 set belongs to class I or II, we used SA methods to actively look for degenerate configurations with varying unit cells, thereby avoiding such issues.

Spin configurations on the underlying 2D square lattice have many more degeneracies than spin configurations on the underlying 1D integer lattice, as can be seen by comparing Fig. 8 with Fig. 1. This massive increase in the number of degeneracies Ω compared to the 1D enumeration can be attributed to the loss of information when going from an *angular-dependent* spin-spin correlation function $\widehat{S}_2(\mathbf{R})$ to an *angular-averaged* radial spin-spin correlation function $S_2(R)$, i.e., for which $\widehat{S}_2(\mathbf{R}) = S_2(|\mathbf{R}|)$ is seldom observed. This isotropy prevents $S_2(R)$ from being able to distinguish spin configurations that only differ through the angular dependence of their spin-spin correlations. Since this property is also shared by other 2D lattices as well as higher-dimensional lattices, it makes the square lattice much more representative of what to expect for such lattices.

The classification for all iso-S_2 sets on the underlying 2D square lattice with $1 \leqslant m \leqslant n \leqslant 5$, as well as $1 \leqslant m \leqslant 3$ and $n = 6$ is shown in Table III. Just as the 1D iso-S_2 sets are more likely to be in class III when they have a large basis (see Fig. 2), the proportion of 2D iso-S_2 sets in class III increases when either m or n is increased. The number of class II iso-S_2 sets also shows the same behavior, since only two of the largest bases for which we have enumerated (3×6 and 5×5) allows for more than two class II iso-S_2 sets. However, a peculiar phenomenon that we have observed is that the number of class I iso-S_2 sets in some system sizes is actually lower than the number of class I iso-S_2 sets in strictly smaller systems, even though the total number of iso-S_2 sets is greater in the former case. For example, there are two times as many class I iso-S_2 sets among 2×3 spin configurations than among 3×3 spin configurations, three times as many class I iso-S_2 sets among 3×4 spin configurations than among 4×4 spin configurations, and four times as many class I iso-S_2 sets among 4×5 spin configurations than among 5×5 spin configurations. In all of these cases, the system size with the lower number of class I iso-S_2 sets is square (i.e., $m = n$), which indicates that the increased symmetry associated with these system sizes actually disfavors the occurrence of class I

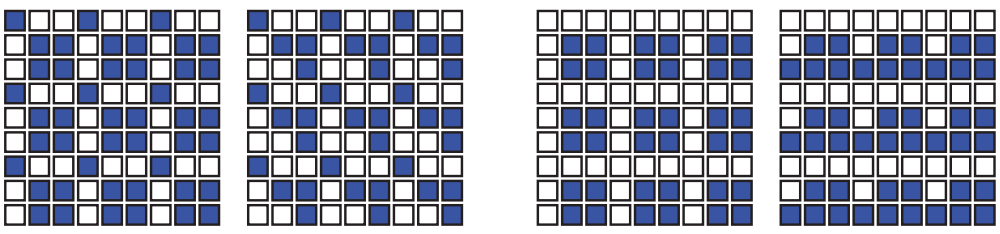

(a) (b)

FIG. 10. (Color online) The two class II iso-S_2 sets containing spin configurations which can be represented using a 3×3 basis on the 2D square lattice. The spin configuration on the left of (a) was previously reported in Ref. 1 as CB[1,2].

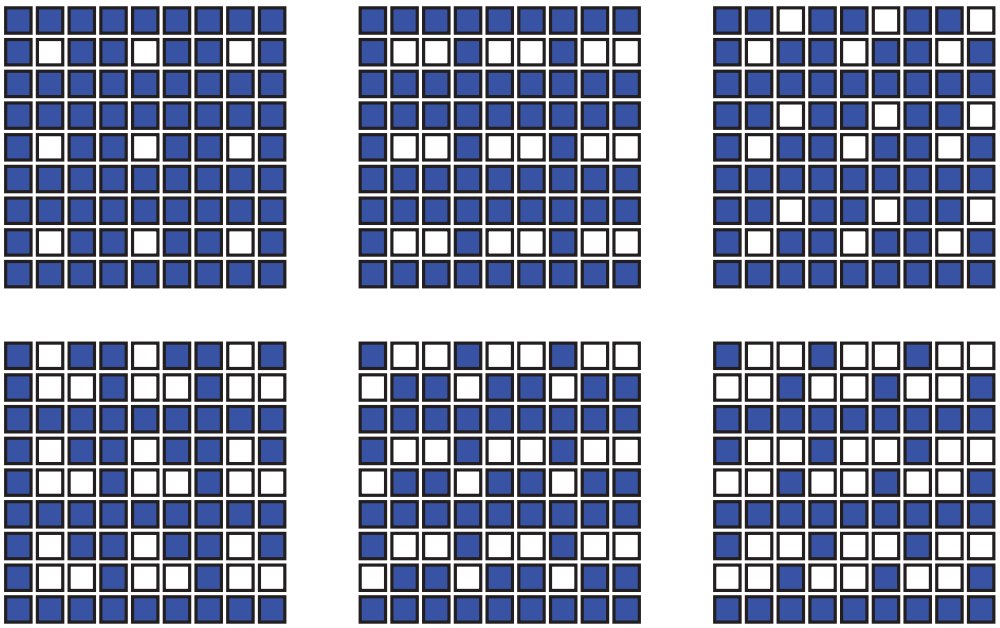

FIG. 11. (Color online) All class III spin configurations which can be represented using a 3×3 basis on the 2D square lattice.

iso-S_2 sets. A subset of the classified sets is also presented in Figs. 9–15.

Unlike the 1D integer lattice case, in which the linear size of the fundamental cell (equal to the number of spins N_F inside of it) is a natural quantity to represent the extent of the smallest periodically replicated unit of a spin configuration, the 2D square lattice has no such quantity. While $\sqrt{N_F}$ could be used, it cannot distinguishes elongated fundamental cells and square

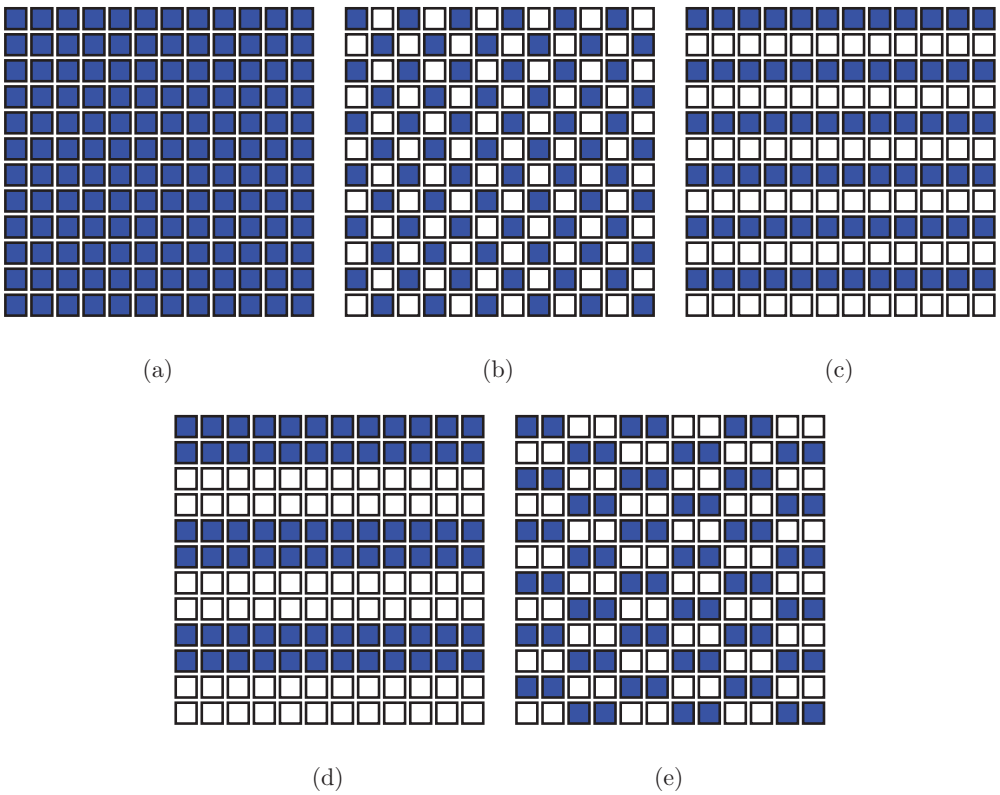

FIG. 12. (Color online) All class I spin configurations which can be represented using a 4×4 basis on the 2D square lattice. All of these spin configurations have been previously reported in Ref. 1 as (a) FM, (b) CB[1,1] (the classic antiferromagnetic ground state), (c) SP[1,1], (d) SP[2,2], and (e) SC[2,2].

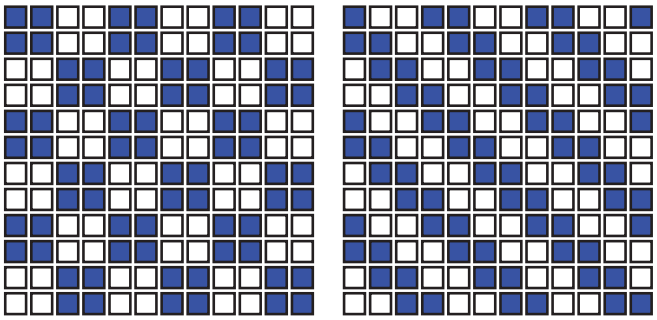

FIG. 13. (Color online) The single class II iso-S_2 set which contains spin configurations which can be represented using a 4×4 basis on the 2D square lattice. This set was previously reported in Ref. 1 as the $\mathbf{CB}_{00}[2,2]$ and $\mathbf{CB}_{11}[2,2]$ block checkerboard spin configurations.

fundamental cells. Instead, we find the two shortest possible lattice vectors (with the second restricted to be noncollinear with the first), and use the length λ_2 of the larger of the two lattice vectors as a representative length of the fundamental cell. An example of how λ_2 is calculated is shown in Fig. 16. Figure 17 compares the λ_2 value of spin configurations with the minimal potential cutoff R_C required to stabilize these configurations on an underlying 2D square lattice. A major difference with the underlying 1D integer lattice is that there is no upper bound at $R_C = \lambda_2$. This is because the reasoning behind the upper bound of R_C for the 1D integer lattice case depended on $S_2(R)$ being equal to its maximal value when R is equal to the configuration period, which is not true in general for the 2D square lattice. There are even some spin configurations for which $S_2(R)$ never reaches its maximum (or minimum) value, such as most of those with a 5×5 basis. An example of a spin configuration with an unusually large R_C for its λ_2 value is shown in Fig. 18, and its corresponding spin-spin interaction potential is presented in Table IV. Despite these differences, both the 1D and 2D spin configurations show an increased required potential range as their fundamental cells grow larger, as expected.

Again, one benefit of enumerating all of the spin configurations (up to some size limit) that are ground states of some spin-spin interaction potential is that such an investigation allows us to discover the limits of what these radial interaction potentials can or cannot stabilize. One question is whether or not one can stabilize spin configurations in which the vast majority of the spins have a given orientation (but not all of them as in the case of the ferromagnetic spin configuration). This is equivalent to asking how close the magnetization per spin of a given spin configuration can be to 1, without actually being 1 (with the magnetization $\langle\sigma\rangle$ of a configuration defined as the averaged value of all the spin values σ_i). The only spin configuration with a magnetization of 1 is the class I ferromagnetic spin configuration, where all spins have identical orientation. It should be mentioned that while some class I striped phase and some class II block checkerboard spin configurations previously studied in Ref. 1 can have a magnetization arbitrarily close to 1, such spin configurations would require very large unit cells. From Table V, we observe that class II sets are highly concentrated at low magnetization. This is a direct consequence of lower magnetization sets having higher degeneracies than higher magnetization sets. Figure 19 shows both $|\langle\sigma\rangle| = 0.6$ class I sets, which are the two class I sets with highest magnetization that we have found during the enumeration process. Table VI contains the spin-spin interaction potentials that stabilize these high magnetization sets.

IV. DISCUSSION AND CONCLUSIONS

The primary goal of the research presented herein was to utilize recently developed inverse statistical-mechanical techniques to (i) enumerate the ground-state spin configurations of the radial pairwise spin-spin interaction potential given in Eq. (1) and (ii) classify these spin configurations according to the solution class designations introduced in Ref. 1. Governed only by computational feasibility, this study focused on spin configurations discretized on the underlying 1D integer and 2D square lattices. In particular, we have found that, with the exception of the smallest system sizes, the majority of target spin configurations can only be ground states with non-S_2-type degeneracies, i.e., they belong to class III iso-S_2 sets. This is in stark contrast to previous papers using inverse methods for point particles interacting according to pairwise radial interactions, which have reported successful uses of the methods to stabilize a wide variety of configurations such as the square, honeycomb, and kagomé crystals in two dimensions,[2,7,29] and the simple cubic, diamond, wurtzite, and calcium fluoride crystals in three dimensions,[4,30–33] but have not reported any configurations which cannot be stabilized using the class of potentials under consideration. While stabilizing such structures is no easy feat, our results open questions about whether the reason why these configurations could be stabilized is simply a consequence of them being relatively simple structures (having only up to 4-particle bases) with a high degree of symmetry or order. Therefore it would be of considerable interest to explore whether or not more complex point-particle configurations can be stabilized by a pairwise radial potential, i.e., whether they would belong to class I or III for such interactions. Additionally, it would be fascinating to see if class II point-particle configurations exist. While the existence of degenerate point-particle configurations is already known (and any degenerate spin configurations can be converted into degenerate point-particle configurations), it is likely that such configurations can be stable ground states of some pairwise radial potential; however, they have yet to be discovered.

One interpretation as to why some spin configurations are in class III instead of being in either class I or II is that the class III configurations are more "complex" or less "ordered" according to some metric. While we have not attempted to define any such metric, our results do not show any indication that would point toward the existence of such a metric beyond the number of spins in the fundamental cell. Configurations with smaller unit cells are indeed more likely to be in class I or II than configurations with larger unit cells, a result that is consistent with our conjecture in Ref. 1 that the fraction of class I configurations goes to zero in the infinite-system limit. Furthermore, for a given system size, configurations

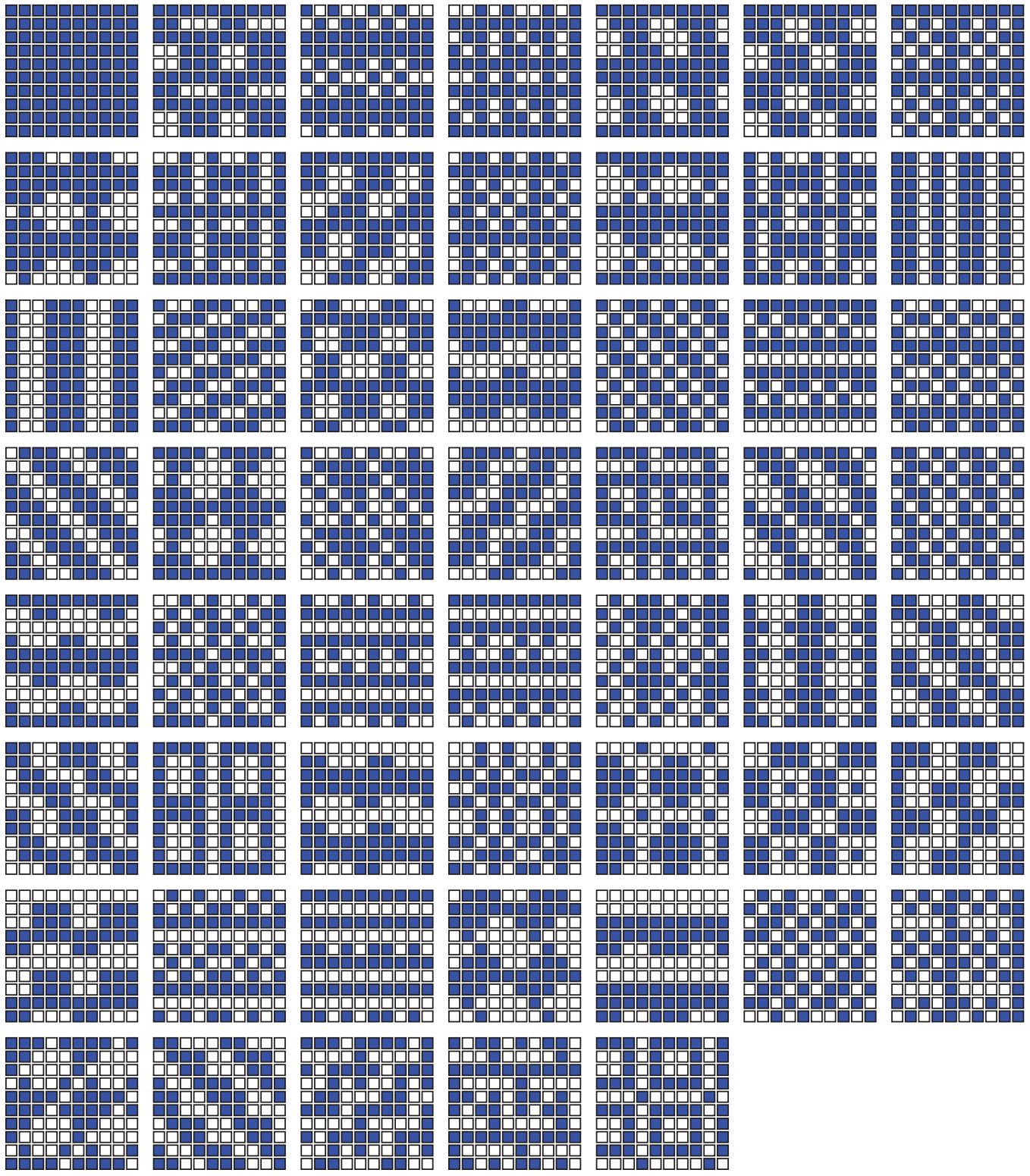

FIG. 14. (Color online) All class I spin configurations which can be represented using a 5×5 basis on the 2D square lattice and are left invariant under some combination of symmetry operations (translations, rotations, reflections, and spin-inversion) besides that which is guaranteed by the underlying 5×5 periodic boundary conditions, displayed left-to-right, top-to-bottom, in order of decreasing absolute magnetization $|\langle\sigma\rangle|$. There are 54 such configurations.

with near-zero magnetization are more likely to be in class I or II than configurations with higher magnetization (see Table V). Besides these two observed trends, it does not seem that there is any other link between the complexity of a given spin configuration and its solution class. Indeed, there are many class I configurations that are devoid of symmetry (besides the

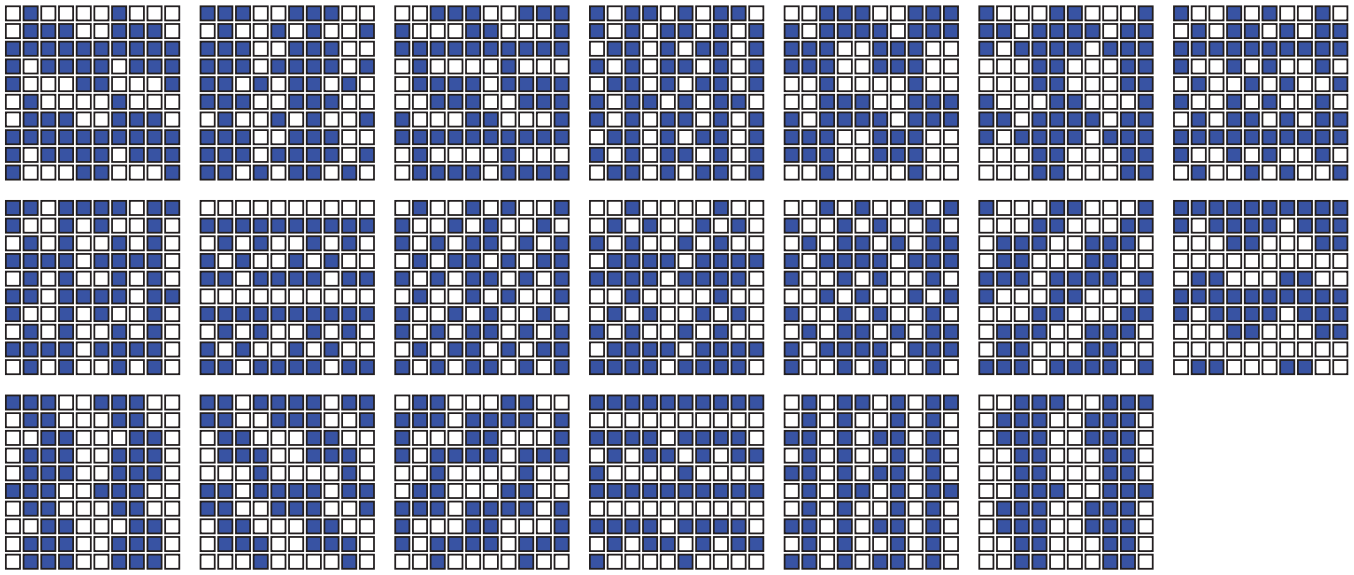

FIG. 15. (Color online) All class I spin configurations which can be represented using a 5×5 basis on the 2D square lattice and are *not* left invariant under any combination of symmetry operations besides that which is guaranteed by the underlying 5×5 periodic boundary conditions, displayed left-to-right, top-to-bottom, in order of decreasing absolute magnetization $|\langle\sigma\rangle|$. There are 20 such configurations.

symmetry resulting from their periodic boundary conditions, compare the spin configurations given in Figs. 14 and 15), while there are also many class III configurations that are more symmetrical. Since class I and II configurations can be mapped to the vertices of a k-dimensional polytope of all allowed values of $S_2(R)$ (c.f. Fig. 11 of Ref. 1), where k is the number of coordination shells for the underlying lattice within the cutoff radius R_C, studying this polytope could lead to an understanding of why certain configurations can be stabilized while others cannot. Additionally, such a study could result in the discovery of a "complexity" or "order" metric which would be a better predictor of the solution class for a given spin configuration. Even if we have no such metric, it is remarkable that we have been able to discover sets of spin configurations which can be unique ground states with some degree of nontrivial degeneracies (i.e., they belong to class II), that are much simpler and more ordered than other well-known disordered degenerate spin configurations.[34–36]

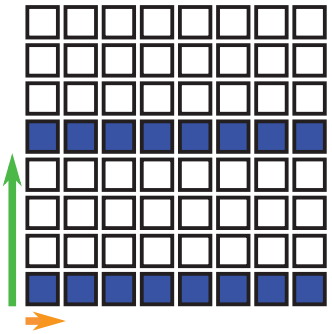

FIG. 16. (Color online) An example demonstrating how λ_2 is calculated for a periodic spin configuration. The arrows denote the two shortest noncollinear lattice vectors of the fundamental cell. Since the lengths of these two vectors are 1 and 4, $\lambda_2 = 4$ (the larger of the two lengths).

Taking advantage of the underlying lattice structure, we were able to determine the shortest range of possible potentials that still correspond to specific target spin configurations as corresponding ground states. For periodic solutions on the 1D integer lattice, the shortest potential cutoff R_C was shown to have an upper bound that is linear in terms of the fundamental cell size. On the other hand, our results are insufficient to conclude whether a lower bound on R_C depends linearly or logarithmically on the fundamental cell size. While periodic solutions on the 2D square lattice also show an increase in lower and upper bounds on R_C with increased λ_2, our data is still too sparse to make any conclusive predictions for larger systems.

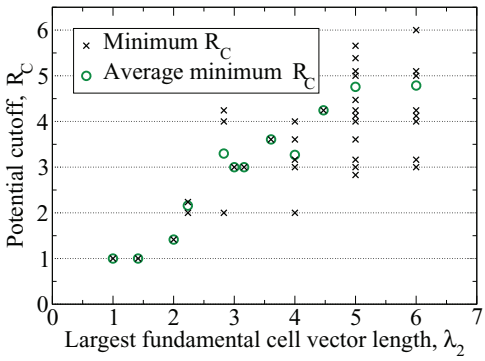

FIG. 17. (Color online) The minimal range R_C of the spin-spin interaction potentials required to stabilize spin configurations on the 2D square lattice in term of the length of the longer lattice vector λ_2 of their fundamental cells. The circles indicate the average R_C for all spin configurations with the same λ_2. It should be mentioned that not all configurations with $\lambda_2 \leqslant 6$ have been considered in this work. Therefore this figure should only be taken as a rough indicator of the range of R_C vs λ_2.

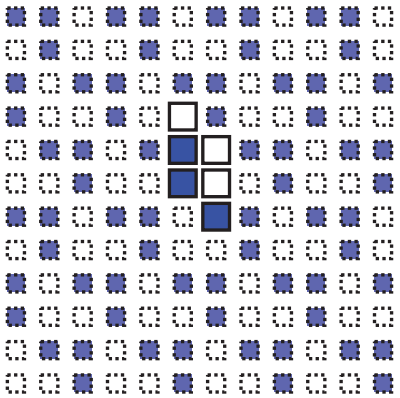

FIG. 18. (Color online) One of the two spin configurations with $\lambda_2 = \sqrt{8}$ that can be stabilized using a spin-spin interaction potential with a minimal cutoff $R_C = \sqrt{18}$. While this configuration is in class I, the other configuration with $\lambda_2 = \sqrt{8}$ and $R_C = \sqrt{18}$ is in class II due to being S_2-degenerate with two other spin configurations with larger fundamental cells. The spins in the fundamental cell are denoted using a solid outline, while other spins are denoted using a dashed outline and smaller squares. The fundamental cell lattice vectors are (1,2) and (−2,2).

The generalized Ising model has several interesting ties to two-phase reconstruction problems, which consist of attempting to recover a two-phase configuration (black and white pixels or voxels) with limited statistical information, such as the standard two-point correlation function.[37–40] It was shown that even if one obtains a configuration with an identical two-point correlation function (analogous to the class II solutions considered in this work), that configuration can be very different from the targeted configuration, as measured by other correlation functions. Additionally, using a correlation function that is analogous to $S_2(R)$, Gommes *et al.*[41] demonstrated that a target configuration can possess an enormous number of degeneracies (e.g., $\sim 10^7$ degeneracies for a disordered 8×8 pattern), which likely grows exponentially with system size. While this number includes both trivial and nontrivial degeneracies, it still indicates that there is a huge number of nontrivial degeneracies. While that study did not distinguish between class I, II, and III solutions, it would not be surprising if this increased number of degeneracies is also the case for class I and II sets.

Given the limitations of achieving unique ground-state spin configurations with radial interactions of finite range, a natural extension of the present application of inverse statistical mechanical techniques is to examine more general spin interactions that would enable one to increase the relative size of the set of class I solutions. One such possible generalization includes directional pairwise spin-spin interactions of finite range, which we expect will dramatically increase the number of possible class I solutions due to the fact that the directional spin-spin correlation function in Eq. (8) more uniquely specifies a target configuration than a radial one.[40]

TABLE IV. The spin-spin interaction potential $J(R)$ corresponding to the spin configuration shown in Fig. 18. The spin-spin correlation function $S_2(R)$, its maximum value on $\mathbb{Z}^2$, $S_2^{\max}(R)$, and the energy per spin ϵ of the ground state are also shown for comparison. Even though the fundamental cell lattice vectors are of length $\sqrt{5}$ and $\sqrt{8}$, $S_2(R)$ is not maximal for either of these distances.

R	$J(R)$	$S_2(R)$	$S_2^{\max}(R)$
1	0.204	$-2/3$	2
$\sqrt{2}$	−0.105	0	2
2	−1	$-2/3$	2
$\sqrt{5}$	1	$2/3$	4
$\sqrt{8}$	0.645	$2/3$	2
3	1	$4/3$	2
$\sqrt{10}$	−0.813	$-4/3$	4
$\sqrt{13}$	0.523	$-4/3$	4
4	−1	$-2/3$	2
$\sqrt{17}$	−0.395	$2/3$	4
$\sqrt{18}$	−1	$2/3$	2
ϵ	−3.084		

TABLE V. The number of (a) 4×5 and (b) 5×5 iso-S_2 sets in each class in term of the absolute magnetization $|\langle\sigma\rangle|$ of the set. It should be noted that all configurations in a given iso-S_2 set have the same magnetization up to a sign.

(a)				(b)			
$\lvert\langle\sigma\rangle\rvert$	I	II	III	$\lvert\langle\sigma\rangle\rvert$	I	II	III
0.0	98	2	879	0.04	28	25	1737
0.1	52	0	1321	0.12	16	4	1690
0.2	82	0	1036	0.20	17	0	1415
0.3	40	0	703	0.28	4	0	1226
0.4	24	0	415	0.36	4	0	903
0.5	2	0	193	0.44	4	0	623
0.6	2	0	87	0.52	0	0	357
0.7	0	0	23	0.60	0	0	169
0.8	0	0	8	0.68	0	0	64
0.9	0	0	1	0.76	0	0	19
1.0	1	0	0	0.84	0	0	5
				0.92	0	0	1
				1.00	1	0	0

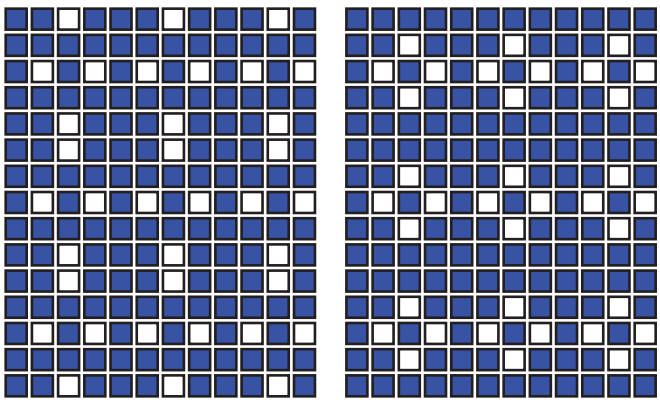

FIG. 19. (Color online) Spin configurations from the two class I iso-S_2 sets with the highest absolute magnetization, $\langle\sigma\rangle = 0.6$, found by our exhaustive search (not considering the ferromagnetic state with $\langle\sigma\rangle = 1$). Both of these spin configurations can be realized using a 4×5 unit cell.

TABLE VI. The spin-spin interaction potentials $J(R)$ corresponding to the spin configurations shown in Fig. 19. The spin-spin correlation function $S_2(R)$, its maximum value on $\mathbb{Z}^2$, $S_2^{\max}(R)$, and the energy per spin ϵ of the ground states are also shown for comparison.

R	$J(R)$	$S_2(R)$	$J(R)$	$S_2(R)$	$S_2^{\max}(R)$
1	−0.108	3/5	−0.318	2/5	2
$\sqrt{2}$	−1	2/5	1	6/5	2
2	−0.201	4/5	−0.486	1	2
$\sqrt{5}$	−0.408	8/5	0.131	4/5	4
$\sqrt{8}$	−0.116	2/5	−0.556	2/5	2
3	−0.620	2/5	0.063	3/5	2
$\sqrt{10}$	0.540	8/5	0.369	8/5	4
$\sqrt{13}$	0.243	8/5	−0.126	4/5	4
4	0.705	7/5	0	6/5	2
$\sqrt{17}$	−0.075	6/5	0.122	8/5	4
$\sqrt{18}$	−0.060	6/5	−0.129	2/5	2
$\sqrt{20}$	−0.022	4/5	. . .	. . .	4
5	0.310	2	. . .	. . .	6
$\sqrt{26}$	0.204	4/5	. . .	. . .	4
$\sqrt{29}$	0.173	12/5	. . .	. . .	4
ϵ	−1.687		−1.140		

Another way to achieve this goal would be to allow not only spin-spin interactions but intrinsic n-spin interactions ($n \geqslant 3$). It would be interesting to investigate the improvement provided by the simplest extension of this type, i.e., directional pairwise and triplet spin interactions.

In addition, it would be equally interesting to investigate spin configurations discretized on other underlying lattices, such as the 2D triangular and 3D cubic lattices. In particular, the 2D triangular lattice is known to have degenerate ground states for the nearest-neighbor antiferromagnetic potential;[22] therefore we expect that this choice of underlying lattice could lead to qualitatively different results than those found in this work with the 2D square lattice.

In future work, it will also be interesting to study the excited states of the spin-spin interactions that led to the various degenerate or nondegenerate ground states identified in this paper. Investigating the phase transition properties of such interactions would be worth comparing to the same properties for other spin-spin interactions, such as those that are position- and orientation-dependent.[42] Allowance for such nonradial interactions in inverse methodologies would make it substantially easier to achieve a given target spin configuration as a unique ground state and enable one to obtain more exotic ground-state structures than with radial interactions alone, as has recently been shown in the case of many-particle systems subject to directional pair potentials.[43]

ACKNOWLEDGMENTS

E.M., F.H.S., and S.T. were supported by the Office of Basic Energy Science, Division of Materials Science and Engineering under Award No. DE-FG02-04-ER46108. R.A.D. received funding from the Department of Energy under Grant No. DE-SC0005180. This work was partially supported by a grant from the Simons Foundation (Grant No. 231015 to S.T.).

[1] R. A. DiStasio, Jr., É. Marcotte, R. Car, F. H. Stillinger, and S. Torquato, Phys. Rev. B **88**, 134104 (2013).
[2] M. C. Rechtsman, F. H. Stillinger, and S. Torquato, Phys. Rev. Lett. **95**, 228301 (2005); **97**, 239901(E) (2006).
[3] M. C. Rechtsman, F. H. Stillinger, and S. Torquato, Phys. Rev. E **73**, 011406 (2006).
[4] M. C. Rechtsman, F. H. Stillinger, and S. Torquato, Phys. Rev. E **75**, 031403 (2007).
[5] S. Torquato, Soft Matter **5**, 1157 (2009).
[6] H. Cohn and A. Kumar, Proc. Natl. Acad. Sci. USA **106**, 9570 (2009).
[7] É. Marcotte, F. H. Stillinger, and S. Torquato, Soft Matter **7**, 2332 (2011).
[8] E. Ising, Z. Phys. **31**, 253 (1925).
[9] B. M. McCoy and T. T. Wu, *The Two-Dimensional Ising Model* (Harvard University Press, Cambridge, 1973).
[10] L. Onsager, Phys. Rev. **65**, 117 (1944).
[11] C. N. Yang, Phys. Rev. **85**, 808 (1952).
[12] K. Barros, P. L. Krapivsky, and S. Redner, Phys. Rev. E **80**, 040101 (2009).
[13] A. J. F. Siegert and David J. Vezzetti, J. Math. Phys. **9**, 2173 (1968).
[14] R. J. Elliott, Phys. Rev. **124**, 346 (1961).
[15] M. E. Fisher and W. Selke, Phys. Rev. Lett. **44**, 1502 (1980).
[16] R. J. Baxter, *Exactly Solved Models in Statistical Mechanics* (Academic Press, London, 1982).
[17] A. Giuliani, J. L. Lebowitz, and E. H. Lieb, Phys. Rev. B **74**, 064420 (2006).
[18] A. Giuliani, J. L. Lebowitz, and E. H. Lieb, Phys. Rev. B **76**, 184426 (2007).
[19] A. Giuliani, J. L. Lebowitz, and E. H. Lieb, Phys. Rev. B **84**, 064205 (2011).
[20] In the summation in Eq. (1), the index i runs over the N spins contained in the unit cell, while the index j runs over spins contained in the unit cell as well as its periodic images.
[21] A generalized Kronecker delta is defined as

$$\delta_{\alpha,\beta} \equiv \begin{cases} 1, & \text{if} \quad \alpha = \beta, \\ 0, & \text{if} \quad \alpha \neq \beta, \end{cases} \tag{10}$$

where α and β are either distances or vectors.
[22] G. H. Wannier, Phys. Rev. **79**, 357 (1950).
[23] K. Kano and S. Naya, Prog. Theor. Phys. **10**, 158 (1953).
[24] J. Oitmaa, J. Phys. A: Math. Gen. **14**, 1159 (1981).
[25] J. Oitmaa, J. Phys. A: Math. Gen. **15**, 573 (1982).
[26] R. Rietman, B. Nienhuis, and J. Oitmaa, J. Phys. A: Math. Gen. **25**, 6577 (1992).
[27] C. C. Wu, J. Stat. Phys. **85**, 251 (1996).

[28]C.-K. Hu and N. S. Izmailian, Phys. Rev. E **58**, 1644 (1998).
[29]E. Edlund, O. Lindgren, and M. N. Jacobi, Phys. Rev. Lett. **107**, 085503 (2011).
[30]M. C. Rechtsman, F. H. Stillinger, and S. Torquato, Phys. Rev. E **74**, 021404 (2006).
[31]É. Marcotte, F. H. Stillinger, and S. Torquato, J. Chem. Phys. **138**, 061101 (2013).
[32]A. Jain, J. R. Errington, and T. M. Truskett, Soft Matter **9**, 3866 (2013).
[33]G. Zhang, F. H. Stillinger, and S. Torquato, Phys. Rev. E **88**, 042309 (2013).
[34]J. Snyder, J. S. Slusky, R. J. Cava, and P. Schiffer, Nature (London) **413**, 48 (2001).
[35]S. V. Isakov, R. Moessner, and S. L. Sondhi, Phys. Rev. Lett. **95**, 217201 (2005).
[36]C. L. Henley, Annu. Rev. Condens. Matter Phys. **1**, 179 (2010).
[37]C. L. Y. Yeong and S. Torquato, Phys. Rev. E **57**, 495 (1998).
[38]M. S. Talukdar, O. Torsaeter, and M. A. Ioannidis, J. Colloid Interface Sci. **248**, 419 (2002).
[39]M. E. Kainourgiakis, E. S. Kikkinides, A. Galani, G. C. Charalambopoulou, and A. K. Stubos, Transport Porous Med. **58**, 43 (2005).
[40]Y. Jiao, F. H. Stillinger, and S. Torquato, Phys. Rev. E **82**, 011106 (2010).
[41]C. J. Gommes, Y. Jiao, and S. Torquato, Phys. Rev. E **85**, 051140 (2012).
[42]H. Au-Yang and B. M. McCoy, Phys. Rev. B **10**, 886 (1974).
[43]S. Martis, É. Marcotte, F. H. Stillinger, and S. Torquato, J. Stat. Phys. **150**, 414 (2013).